May, 15th 2018, Nürnberg, Germany

Spatial distribution of nucleated bubbles in molten glasses undergoing coalescence and growth

D. Boloré (Surface du Verre et Interfaces, UMR 125 CNRS/Saint-Gobain)
& F. Pigeonneau

Industrial Context

- Cullet is mainly used for the production of container glass:

Germany	85 %	Belgium	96 %	France	75 %
Poland	**57** %	Italy	78 %	Austria	87 %
United-Kingdom	66 %	Portugal	58 %	Spain	70 %
Sweden	**99** %	Holland	83 %	Denmark	85 %

Table 1: Rates of glass recycling in Europe in 2015 [FEVE source].

- Advantages of introduction of cullet in raw materials:
  - Reductions of mineral resources;
  - Reduction of CO_2 release;
  - Reduction of the energy to provide.

Industrial Context

- Cullet is mainly used for the production of container glass:

Germany	85 %	Belgium	96 %	France	75 %
Poland	**57** %	Italy	78 %	Austria	87 %
United-Kingdom	66 %	Portugal	58 %	Spain	70 %
Sweden	**99** %	Holland	83 %	Denmark	85 %

Table 1: Rates of glass recycling in Europe in 2015 [FEVE source].

- Advantages of introduction of cullet in raw materials:
  - Reductions of mineral resources;
  - Reduction of CO_2 release;
  - Reduction of the energy to provide.

What is the limitation to reach 100 % of cullet?

Industrial Context

Industrial Context

How and why these bubbles are created?

1. Experimental set-up
2. Spatial distributions of nucleated bubbles
3. Bubble growth rate
4. Saturation and nucleation
5. Conclusion

1. Experimental set-up

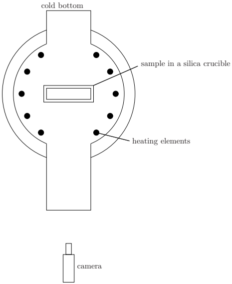

Figure 1: Sketch of HTO furnace.

SiO_2	Na_2O	CaO	MgO	Al_2O_3	SO_3	Fe_2O_3	FeO
72.4	13.85	8.88	3.74	0.73	0.22	0.055	0.014

Table 2: Composition of the **float glass** (wt %).

- Recording of the melting with 2 cameras (60 and 25 $\mu m/px$).

2. Spatial distributions of nucleated bubbles

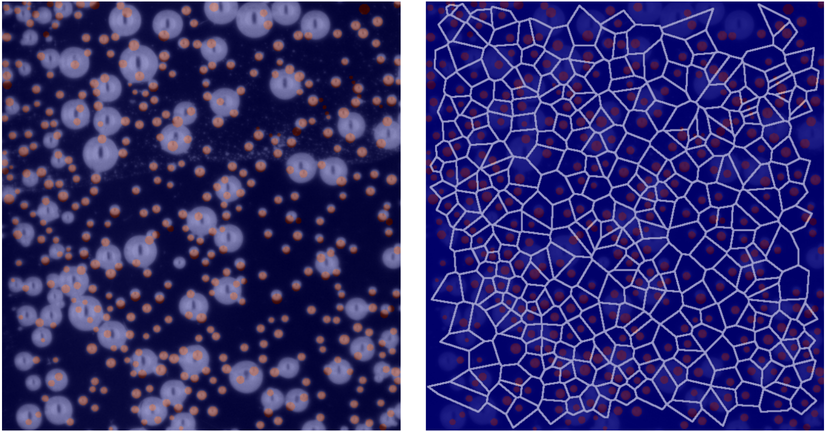

Figure 2: Detection of nucleation sites on each face of the crucible and Voronoï diagram of nucleation sites.

2. Spatial distributions of nucleated bubbles

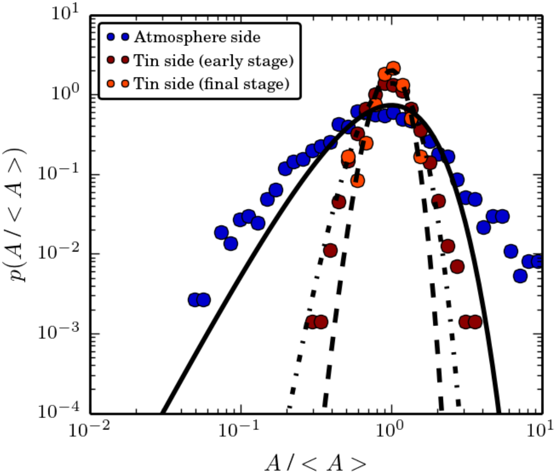

Figure 3: PDF of the area of Voronoï cells.

2. Spatial distributions of nucleated bubbles

- PDF can be described by the Gamma distribution:

$$f(x) = n^n x^{n-1} e^{-nx}/\Gamma(n), \tag{1}$$
$$\text{with } x = \frac{A}{\langle A \rangle}.$$

- Atmosphere side: $n = 3.5$;
- Tin side: $n = 12.2$ at the beginning and $n = 25.5$ at the end.
- For objects randomly distributed over a surface, $n = 7/2$[1].
- The disagreement on the tin side due to the **bubble coalescence**.

[1] J.-S. Ferenc/Z. Néda: On the size distribution of Poisson Voronoi cells, in: Physica A 385.2 (2007), pp. 518–526.

2. Spatial distributions of nucleated bubbles

- Simulation population of bubbles undergoing coalescence:
  1. Population of 3000 “nuclei” distributed following a Poisson distribution over a square of 10^8 pixels;
  2. At each step, the closest “nuclei” are gathered at the barycentre position.

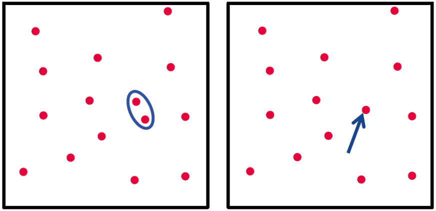

Figure 4: Coalescence between the closest nuclei.

  3. Process is reiterated 500 to 1500 times.
  4. “Numerical experiences” are repeated 500 times.

2. Spatial distributions of nucleated bubbles

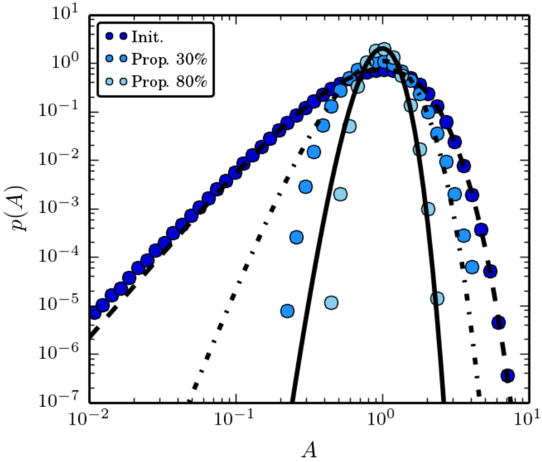

Figure 5: PDF of area of Voronoï cells obtained from the numerical simulations.

2. Spatial distributions of nucleated bubbles

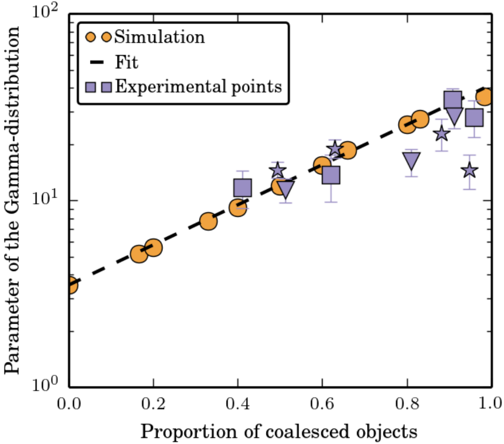

Figure 6: n vs. the proportion of coalesced objects.

$$n = \frac{7}{2} e^{2.47x}, \text{ with } x = \frac{d_0 - d}{d_0}. \tag{2}$$

2. Spatial distributions of nucleated bubbles

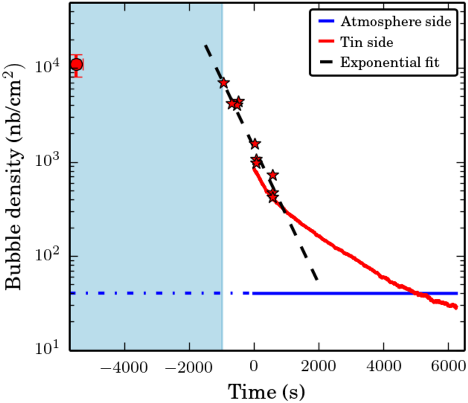

Figure 7: Bubble densities on the two sides of glass samples.

- In atmosphere side, $d_0 = 40$ nuclei/cm^2;
- In tin side, $d_0 = 9300$ nuclei/cm^2 (230 times larger).

3. Bubble growth rate

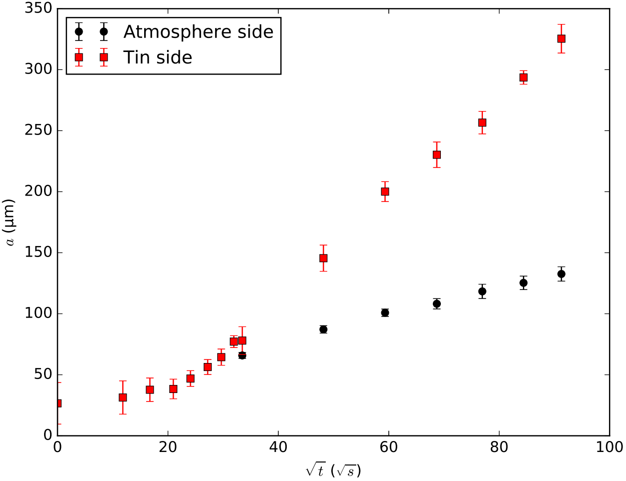

Figure 8: *a* (μm) vs. $\sqrt{t}$ ($\sqrt{\mathrm{s}}$) for bubbles on tin and atmosphere sides of molten glass samples.

3. Bubble growth rate

- Three redox couples are taken into account[2]:

$$Fe^{3+} + \frac{1}{2}O^{2-} \rightleftharpoons Fe^{2+} + \frac{1}{4}O_2, \tag{3}$$

$$SO_4{}^{2-} \rightleftharpoons SO_2 + \frac{1}{4}O_2 + O^{2-}, \tag{4}$$

$$Sn^{4+} + O^{2-} \rightleftharpoons Sn^{2+} + \frac{1}{2}O_2. \tag{5}$$

- Gas contents (O_2, SO_2, H_2O, CO_2 & N_2) and bubble radius are determined by:

$$\frac{dn_{G_j}}{dt} = 4\pi a D_{G_j}(C_{G_j} - L_{G_j} P_{G_j}^{\beta_{G_j}}), \tag{6}$$

$$\frac{da}{dt} = \frac{a}{4\mu}\left(\sum_{i=1}^{N_g} P_{G_i} - P_l - \frac{2\gamma}{a}\right). \tag{7}$$

[2] F. Pigeonneau: Mechanism of mass transfer between a bubble initially composed of oxygen and molten glass, in: Int. J. Heat Mass Transfer 54 (2011), pp. 1448–1455.

3. Bubble growth rate

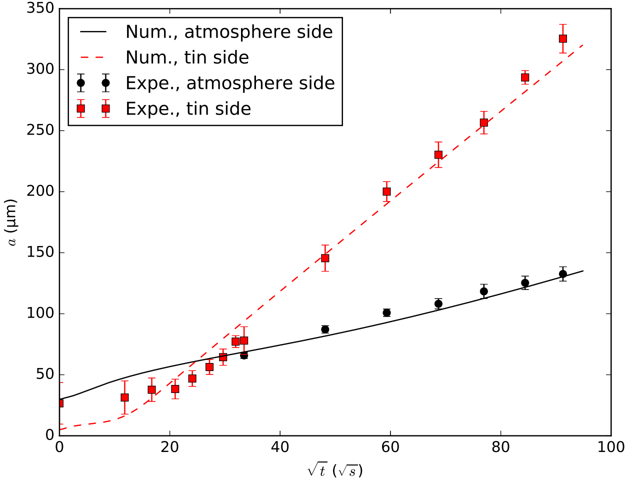

Figure 9: *a* (μm) vs. $\sqrt{t}$ ($\sqrt{\mathrm{s}}$) for bubbles on tin and atmosphere sides of molten glass samples.

3. Bubble growth rate

- In atmosphere side, $P_{O_2} = 1.3 \cdot 10^{-3}$ Pa; tin side, $P_{O_2} = 4.1 \cdot 10^{-4}$ Pa.
- **Tin leads to a reduction of glass.**
- **Decrease of the SO_2 chemical solubility.**

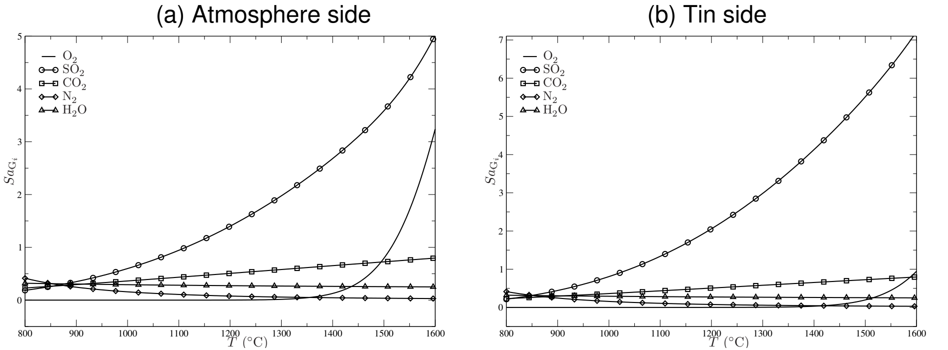

Figure 10: $Sa_{G_i} = C_{G_i}/(L_{G_i} P_l^{\beta_{G_i}})$ of the 5 gas species vs. T on both sides.

4. Saturation and nucleation

- The critical bubble size for nucleation in the case of multi-species is given by

$$a_{\mathrm{cr}} = \frac{2\gamma}{\left(\sum_{i=1}^{N_g} Sa_{\mathrm{G}_i}^{1/\beta_{\mathrm{G}_i}} - 1\right) P_l}, \tag{8}$$

$$Sa_{\mathrm{G}_i} = \frac{C_{\mathrm{G}_i}}{L_{\mathrm{G}_i} P_l^{\beta_{\mathrm{G}_i}}}. \tag{9}$$

- The supersaturation for N_g dissolved species is

$$\sigma = \sum_{i=1}^{N_g} Sa_{\mathrm{G}_i}^{1/\beta_{\mathrm{G}_i}} - 1. \tag{10}$$

4. Saturation and nucleation

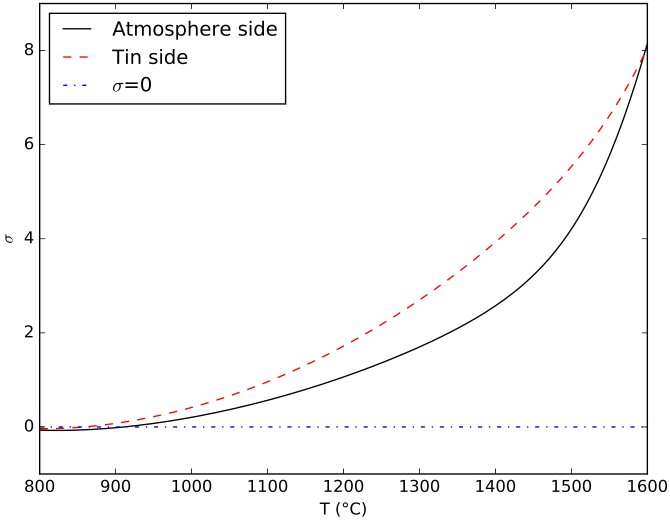

Figure 11: σ vs. T (°C) in atmosphere and tin sides.

5. Conclusion

- Remelting of cullet leads to a large bubble formation.
- Enhancements of the bubble nucleation and growth rate due to the tin pollution.
- The glass reduction on tin side is the main parameter controlling the bubble nucleation and the growth rate.
- Difficult to quantify the bubble nucleation rate (work in progress to improve the prediction).
- The 100 % of cullet is difficult to reach because the bubble creation persists and needs to introduce fining agents.
- See for more details[3].

[3] D. Boloré/F. Pigeonneau: Spatial distribution of nucleated bubbles in molten glasses undergoing coalescence and growth, in: J. Am. Ceram. Soc. 101.5 (2018), pp. 1892–1905.